Characterization and Structure–Property Relationship of Chemical Oxidative Polymerization of Poly(*para*-hydroquinone)

T. Tibaoui,[1] S. Ayachi,[1] M. Hamidi,[2] M. Bouachrine,[2] M. Paris,[3] K. Alimi[1]

[1]*Unité de Recherche, Matériaux Nouveaux et Dispositifs Electroniques Organiques, Département de Physique, Faculté des Sciences de Monastir, Monastir 5000, Tunisie*
[2]*LRMM, Département de Chimie, Faculté des Sciences et Techniques, B. P. 509, Boutalamine, Errachidia, Maroc*
[3]*Institut des Matériaux Jean Rouxel, CNRS-UMR 6502, 2 Rue de la Houssiniére, BP 32229, 44322 Nantes Cédex 3, France*

Received 3 March 2008; accepted 27 July 2009
DOI 10.1002/app.31226
Published online 26 May 2010 in Wiley InterScience (www.interscience.wiley.com).

ABSTRACT: Poly(*para*-hydroquinone) (PPHQ) was prepared by chemical oxidation reaction using titanium tetrachloride ($TiCl_4$) as an oxidant. Solid-state nuclear magnetic resonance (CPMAS ^{13}C-NMR), infrared absorption, optical absorption, thermal analysis (TGA and DTA), and electron paramagnetic resonance techniques were used to characterize the obtained PPHQ polymer. The correlation between different experimental results justifies the chemical structure and proves the vibrational and optical properties of this polymer. Theoretical calculations based on *ab initio* density functional theory and semiempirical Austin Model 1 methods were accomplished to elucidate the structure–property relationship of PPHQ polymer. From oligomer 8-hydroquinone, we have predicted the experimentally observed results. This oligomer is considered as model structure, which reproduces the PPHQ polymer characteristics and elucidates the $TiCl_4$ effect on the properties of the polymer under study. © 2010 Wiley Periodicals, Inc. J Appl Polym Sci 118: 711–720, 2010

Key words: conjugated polymers; FTIR; NMR; calculations; structure–property relations

INTRODUCTION

Poly(*para*-dihydroxy-phenylene) or poly(*p*-hydroquinone) (PPHQ) (Scheme 1), considered as a stable redox polymer, has been prepared via oxidative polycondensation of *p*-benzoquinone in the presence of Lewis acids ($ZnCl_2$, $AlCl_3$, $BF_3.OEt_2$).[1] The aim of previous work was to discover how the nature of the Lewis acids influences the structure, properties, and yield of PPHQ polymer.[1] On the basis of structural analyses (chemical and spectral methods), it was demonstrated that PPHQ possessed semiconducting and electron exchange properties when using Boron trifluoride etherate ($BF_3.OEt_2$) as an oxidant. The electrical conductivity of the pristine polymer ($\sigma = 1.5\ 10^{-12}\ \Omega^{-1}\ cm^{-1}$) is increased up to $\sigma = 5\ 10^{-2}\ \Omega^{-1}\ cm^{-1}$ by doping with iodine in tetrahydrofuran.[2]

As reported by Yamamoto et al.,[3,4] the preparation of a PPHQ film was done through electrooxidative polymerization of hydroquinone. This polymer has shown very interesting optical properties and has been identified as a blue luminescent semiconductor. Then, the absorption and emission wavelengths in *N*,*N*-dimethylformamide are 345 and 420 nm, respectively.

It has been reported that polymers containing hydroquinone units in their main chain present interesting chemical properties.[5] However, to our knowledge, there are few reports in the literature concerning the PPHQ polymerization mechanisms.

On the other hand, it has been shown that density functional theory (DFT) method was in many instances more accurate for predicting polymerization mechanisms.[6,7] Thus, a great deal of experimental and theoretical work related to geometric parameters and optical transitions has been published.[8]

Recently, PPHQ was prepared by chemical oxidation in the presence of titanium tetrachloride ($TiCl_4$) as an oxidant. The resulting amorphous polymer, which is insoluble in common organic solvents,

Correspondence to: K. Alimi (kamel.alimi@fsm.rnu.tn).
Contract grant sponsor: The AUF Organization; contract grant number: 63/3PS589.
Contract grant sponsor: The Tuniso-Marocain Cooperation; contract grant number: 06/TM/81.
Contract grant sponsor: The Tunisian-French Cooperative Action; contract grant number: CMCU/07G1309.

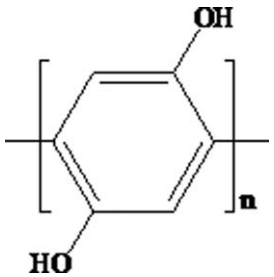

Scheme 1 Chemical structure of PPHQ polymer.

was experimentally studied, in powder form, by solid-state nuclear magnetic resonance (CPMAS ^{13}C-NMR), infrared absorption, optical absorption, thermal analysis (TGA and DTA), and electron paramagnetic resonance (EPR).

In an attempt to describe the polymer structure and to investigate the relationship between structure and properties, we have performed theoretical calculations with *ab initio* based on DFT and semiempirical method using Austin Model 1 (AM1). This combination leads to a better understanding of the $TiCl_4$ effect on the polymer properties.

EXPERIMENTAL AND THEORETICAL DETAILS

Experimental part

The chemical polymerization of hydroquinone with an oxidizing agent, $TiCl_4$, was carried out essentially according to the procedure for the polymerization described in the literature.[9,10] To a solution of hydroquinone (1 g, 0.012 mol) in 100 mL dry chloroform, a solution of anhydrous $TiCl_4$ (9.07 g, 0.048 mol) in 100 mL dry chloroform was added at room temperature. The resulting solution was stirred for about 17 h at room temperature, then poly(2.5-hydroquinone) in doped state in chloroform was obtained, which can be cast into free standing film. The bluish black poly(2.5-hydroquinone) powder was obtained by reprecipitation with about 400 mL of methanol, then successive soxhlet-extraction with methanol and acetone to remove residual oxidant and oligomers. After dedoping with hydrazine, filtration, and washing with methanol, the purified poly(2.5-hydroquinone) (PPHQ) in neutral state was dried in vacuum.

CPMAS ^{13}C-NMR spectrum was acquired at room temperature using a Bruker Avance 500 MHz spectrometer operating at 125.7 MHz for ^{13}C using a 4-mm double-bearing Bruker probehead. All rotors were spun under dry nitrogen flow. Spectrum was referenced to tetramethylsilane for ^{13}C (using adamantane as a secondary reference). {^{1}H}-^{13}C CPMAS (cross-polarization magic-angle spinning) NMR spectrum was acquired using a ramp-amplitude sequence,[11] a 2 ms contact time, a repetition time of 2 s, and a 15 kHz MAS spinning rate. ^{1}H decoupling during acquisition was achieved using the TPPM method[12] with a RF field of $\sim$ 60 kHz. Because of the dipolar interactions occurring in PPHQ polymer, it seems that ^{1}H-NMR spectroscopy is useless in this investigation.

EPR experiments were performed in the temperature range 115–300 K on a Bruker Elexsys 500 spectrometer operating at X band. For recorded powder spectra, an EPR quartz tube was filled to a height of typically 1 cm.

Infrared and optical density spectra were carried out at room temperature using a Brucker Vector 22 spectrophotometer and a Carry 2300 spectrophotometer, respectively. For infrared absorption measurements, band positions are expressed in wave number from 400 to 4000 cm^{-1}. The samples were pellets of KBr mixed with the organic compound under study. The wavelengths, expressed in nm for optical density, vary from 0.62 (2000 nm) to 6.2 eV (200 nm).

Dynamic thermogravimetric analysis was carried out in a Perkin-Elmer TGS-1 thermal balance with a Perkin-Elmer UV-1 temperature program control. Samples were placed in a platinum sample holder, and the thermal degradation measurements were carried out between 300 and 973 K at a speed rate of 5 K/min under air atmosphere.

Theoretical part

First of all, the conformational potential energy surface (PES) for the neutral structure of oligo-hydroquinone was generated with Gaussian 98 package[13] and carried out by changing the torsional angle (θ, dihedral angle between two phenyl rings by a 5° step between 0 (syn-planar) and 180° (anti-planar) within single-point calculations. The geometric parameters, such as bond distances and C—O—H

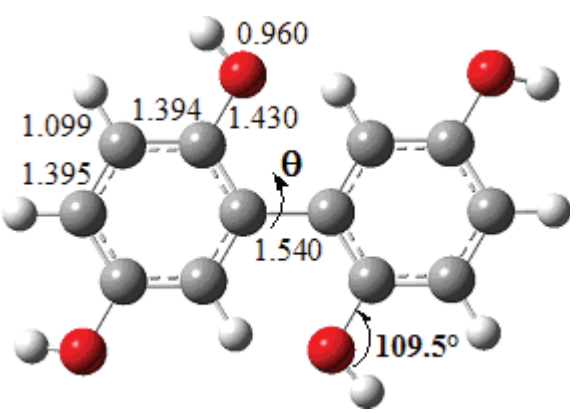

Scheme 2 Geometric parameters of dihydroquinone (the bond lengths are expressed in ångström). [Color figure can be viewed in the online issue, which is available at www.interscience.wiley.com.]

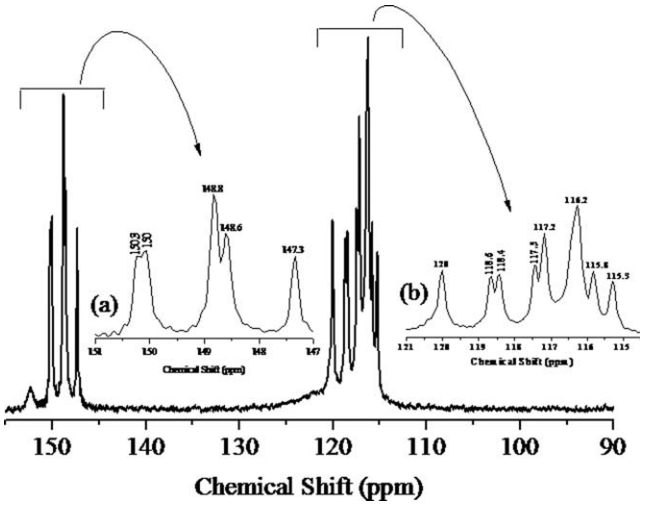

Figure 1 CPMAS ^{13}C-NMR spectrum of PPHQ polymer: (a) the first and (b) the second domains of chemical shift.

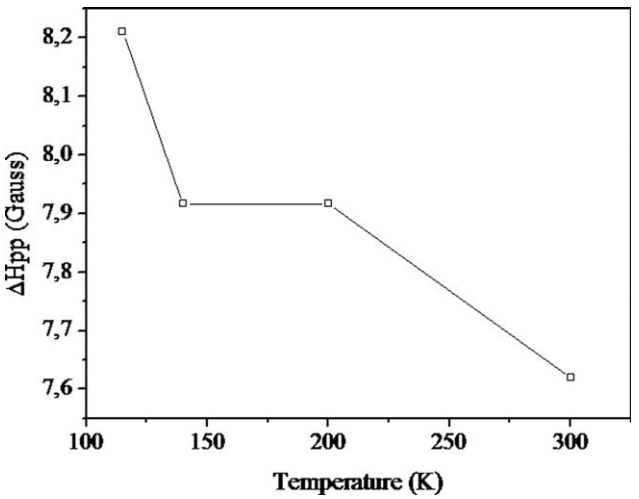

Figure 3 Evolution of peak-to-peak line width (ΔH_{pp}) versus temperature for PPHQ polymer.

angles, have kept fixed (Scheme 2). For each conformation, θ was held fixed, whereas the remaining variables were optimized, that is, no rigid rotor approximation was adopted. The stable molecular geometries, corresponding to the energy minima on PES, were separately obtained by releasing the constraints of the torsional angles, θ. The global energy minimum of each PES was referred to as zero.

Our theoretical calculations are carried out on PHQ oligomers starting from one until nine monomers. In that case, diverse calculations have been performed as follows: (i) starting from structural optimization of the organic material under study, isolated in gas phase (system model), (ii) the identification and characterization of geometrical and structural properties, (iii) the response to the addition of extra charge (interaction with dopant ion), and (iv) the determination of its electronic structure, which is compared to experimental data obtained from optical spectra.

Oligomer geometric structures have been fully optimized using the most popular Becke's three-parameter hybrid functional, B3,[14] with nonlocal correlation of Lee–Yang–Parr, LYP, abbreviated as B3LYP, method.[15] This method, based on DFT for an uniform electron gas (local spin density approximation), is used with the 3-21 G* basis set.[16] In this basis set, d-orbitals have been added to nonhydrogen atoms such as carbon and oxygen. In fact, this basis has been successfully applied to some conjugated polymers systems.[17,18] In parallel, calculations were also performed with Hartree-Fock (HF) method at the same level for comparison purposes.

The DFT/B3LYP/3-21G* and HF/3-21G* methods are implemented in Gaussian 98 program.[13] The electronic properties as HOMO (highest occupied molecular orbital), LUMO (lowest unoccupied molecular orbital) levels and their corresponding

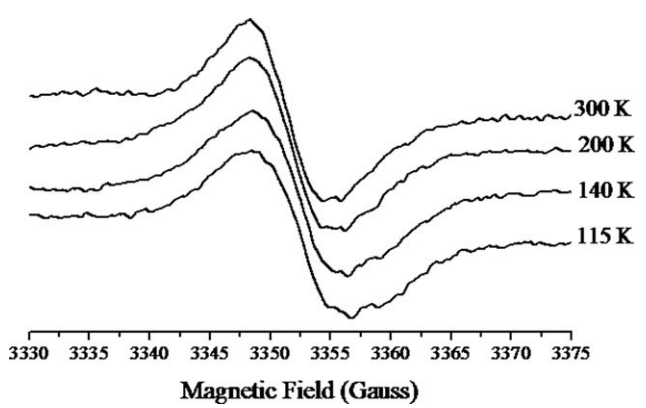

Figure 2 EPR signals of PPHQ polymer at different temperatures.

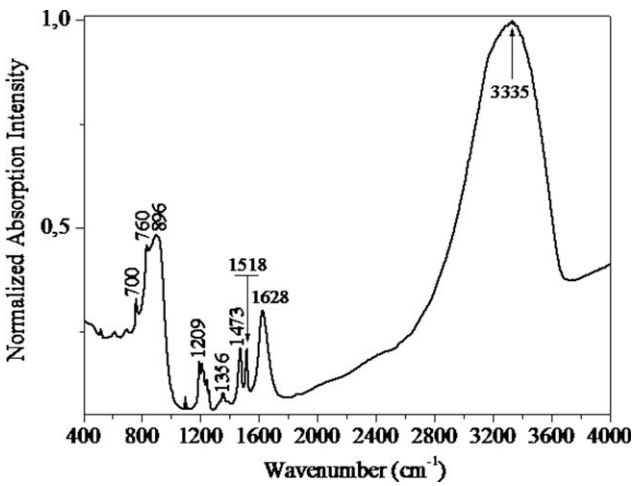

Figure 4 Infrared absorption spectrum of PPHQ polymer.

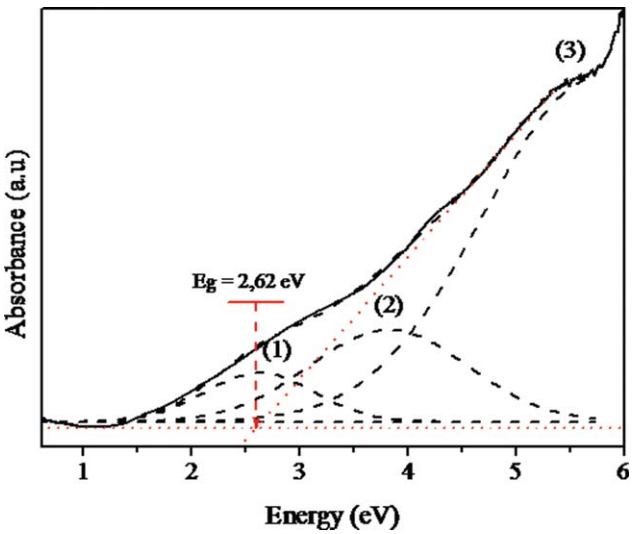

Figure 5 Deconvoluted optical density spectrum of PPHQ polymer. [Color figure can be viewed in the online issue, which is available at www.interscience.wiley.com.]

energetic levels difference for oligomers are also elucidated. Vibrational frequencies calculations have been carried out with semiempirical AM1 method[19] on fully geometry-optimized structure and directly compared to those of infrared absorption measurements. Alternatively, normal coordinate analysis forms have been carried out using Mopac 2000 program.[20] In this method, the matrix of the second derivatives of the energy with respect to displacements of all pairs of atoms in x, y, z directions are calculated. On diagonalization, this provides the force constants for the molecules.

EXPERIMENTAL RESULTS

CPMAS ^{13}C-NMR results

Figure 1 depicts the CPMAS ^{13}C-NMR spectrum of the prepared PPHQ polymer. Quantitatively and through chemical shift, we can note the presence of two different domains. The first one ranging from 115 to 120 ppm [Fig. 1(b)] and the second from 147 to 151 ppm [Fig. 1(a)]. It can be noticed that the peaks of the first domain are attributed to the C—H aromatic and C—C inter-ring. The lines attributed to the hydroxyl groups[21] are consistent with the second domain. Between the two domains, no significant peaks are observed. We later discuss the $TiCl_4$ effect on the structural properties in the Discussion section.

TABLE I
Results of Optical Density Deconvoluted Spectrum

Peak transitions	(1)	(2)	(3)
Peak position (eV)	2.62798	3.82024	5.76412
FWHM	1.02318	1.46989	2.11597
Integrate area	0.29027	0.7832	4.21764

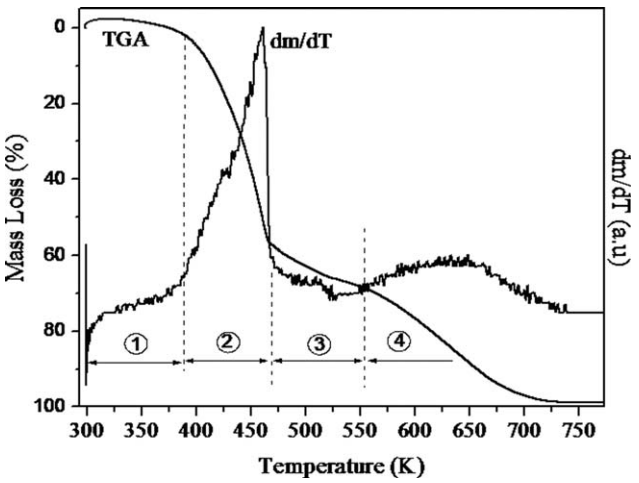

Figure 6 Thermal gravimetric analysis (TGA) and its derivative of PPHQ polymer.

EPR results

In Figure 2, we present the EPR lines evolution under temperature of the PPHQ polymer. Quantitatively, the EPR lines shape is almost the same and not affected by temperature. In a system with free spin charge carrier, one of relaxation mechanisms in EPR is the spin-orbit coupling.[22] This effect could explain the observed broadening of the EPR peak-to-peak line width (ΔH_{pp}) (Fig. 3). As well, we note the increase in the line width with decreasing temperature. This increase is due to electron localization that leads to a reduced motional narrowing or spin diffusion[23] and consequently to the decrease of the spin-orbit coupling.[21] On the other hand, the

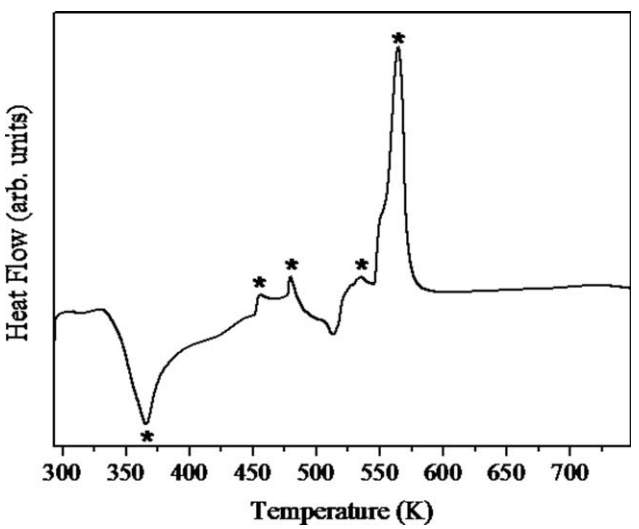

Figure 7 Differential thermal analysis (DTA) of PPHQ polymer.

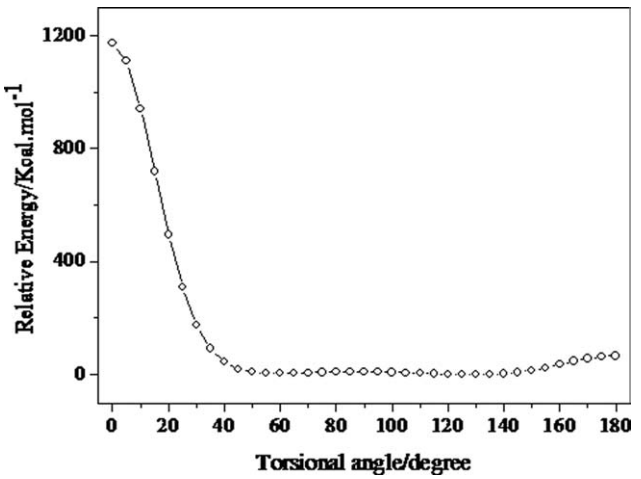

Figure 8 Potential energy curve of PHQ8 as obtained from single-point (SP) calculations.

g-values vary from 2.0032 at 115 K to reach 2.0036 at 300 K. These values indicate that electron localization takes place over a few carbon atoms of the rings.[24] This fact is probably due to the effect of dihydroxyl groups, which generates a steric hindrance.

Infrared absorption results

The infrared absorption spectrum of PPHQ (Fig. 4) consists of the following absorption bands (IR (KBr, cm^{-1})): 760–896 cm^{-1} (ν_{C-H} ring vibration of 1,4-substituted benzene)[25,26]; 1473, 1518, and 1628 cm^{-1} ($\nu_{C=C}$ stretching of the aromatic rings); 1209 cm^{-1} (ν_{C-O} stretching phenol), and 3335 (ν_{O-H} stretching hydroxyl). The presence of these bands may indicate the formation of PPHQ polymer.

Optical absorption measurements

In Figure 5, we show the optical absorption spectrum of PPHQ polymer. The maximum of the absorption band is peaked at ~ 5.70 eV (~ 218 nm), which is ascribed to the π–π* optical transition. This

TABLE II
Optoelectronic Parameters Resorting from DFT Calculations

Compound	Method	ε_{HOMO} (eV)	ε_{LUMO} (eV)	ε_g (eV)
Neutral PHQ8	B3LYP/3-21G*	−4.603	−1.273	3.330
	HF/3-21G*	−6.981	+2.208	4.773
Oxidized PHQ8	B3LYP/3-21G*	−6.764	−3.672	3.092
Neutral PHQ9	B3LYP/3-21G*	−4.582	−1.326	3.256
	HF/3-21G*	−6.927	+2.208	4.719
Oxidized PHQ9	B3LYP/3-21G*	−6.596	−3.542	3.054
Ionization potential (eV)	B3LYP/3-21G*	PHQ8 5.394	PHQ9 5.325	

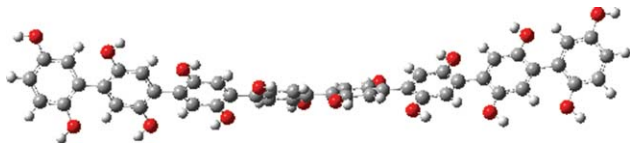

Figure 9 B3LYP/3-21G* optimized structure of the neutral PHQ8 oligomer. [Color figure can be viewed in the online issue, which is available at www.interscience.wiley.com.]

later reflects the polyconjugated backbone of polymer. Besides, the extrapolation of the linear part of the optical absorption, which corresponds to an approximation of the band gap as indicated in Figure 5, was estimated to be 2.62 eV (~ 473 nm). Moreover, UV–vis spectrum can be deconvoluted in three vibronic bands (Fig. 5) using the software origin version 6.0 with the spectrum in eV scale and fitting the peak profile with gaussian functions. Although the deconvolution of the spectra is always an arbitrary procedure, we define the full width at the half maximum (FWHM) and the maximum of the peaks values, either to their corresponding integrate area (Table I).

Thermal analysis

As seen from Figure 6, PPHQ polymer decomposes in four steps. The first one presents the thermal stability of polymer (weight loss less than 5%). A significant second weight loss (from 395 to 465 K) is observed and is related to the disappearance of residual chloroform as a solvent. The two others steps (from 465 until 773 K) correspond to the polymer decomposition. The TGA derivative curve, plotted in the same figure, supports the above observations by the presence of two pronounced peaks indicating the first and the final polymer decomposition.

It can be seen from Figure 7 that there is an endothermic peak at 365.6 K owing to the removal of traces of water trapped by the polymer during weighing of the obtained sample. On the other hand, exothermic peaks appear on the DTA curve in the range 458–538 K, which probably result from the partial oxidation of hydroquinone groups. The most

Figure 10 B3LYP/3-21G* optimized structure of the oxidized PHQ8 oligomer. [Color figure can be viewed in the online issue, which is available at www.interscience.wiley.com.]

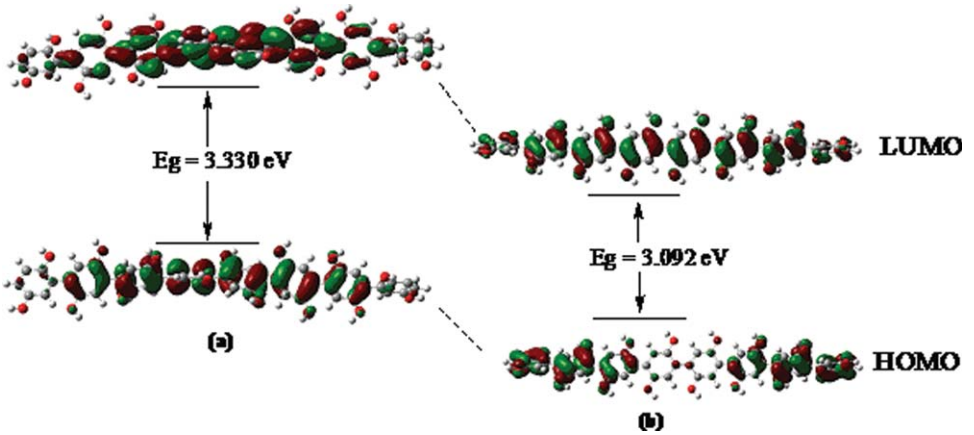

Figure 11 The contour plots of HOMO and LUMO of: (a) neutral and (b) oxidized PHQ8. [Color figure can be viewed in the online issue, which is available at www.interscience.wiley.com.]

relevant exothermic peak, located at 564.6 K, corresponds to dehydroxylation process and to oxidative scission of quinone rings. These observations are in close resemblance to those investigated in literature.[1]

THEORETICAL CALCULATIONS

Conformational analysis

The conformational analysis has been performed for neutral oligo-8-hydroquinone structure (Fig. 8). Hence, two minima at 60° (local minimum) and 130° (global minimum) were identified. Then, our calculation is based on the optimized structure for both neutral and oxidized states with inter-ring dihedral angle of 130°.

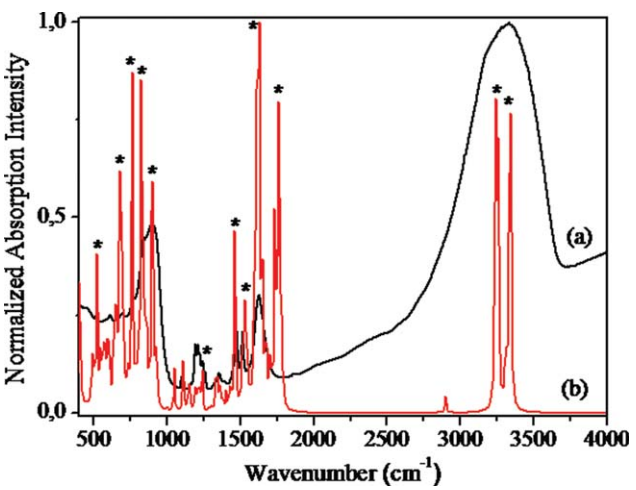

Figure 12 Infrared absorption spectra of PPHQ polymer: (a) experimental and (b) theoretical. [Color figure can be viewed in the online issue, which is available at www.interscience.wiley.com.]

Geometric and electronic structures

Our attempt is to show to what extent the PPHQ polymer properties can be predicted based on extrapolation from oligomer data. Our attention was first focused on the electronic structure, to analyze the location of the HOMO, the LUMO levels and consequently the optical gap of polymer as a result of DFT and HF calculations. For this purpose, we have considered the eight and nine hydroquinone rings. These oligomers are noted PHQ8 and PHQ9, respectively. Using DFT, which is known for a good estimating of band gap values,[27–31] the geometries of these oligomers are fully optimized. For comparison purposes, fully optimized neutral structures were obtained using HF/3-21G* level. The results of calculations were compared with experimental data.

The optoelectronic parameters (ε_{HOMO}, ε_{LUMO}, $\Delta\varepsilon_{LUMO-HOMO}$, and ionization potential) of the two oligomers at the neutral and oxidized states are labeled in Table II.

According to this table, it is interesting to note that similar results are obtained for both oligomers. As a result, we conclude that DFT calculations

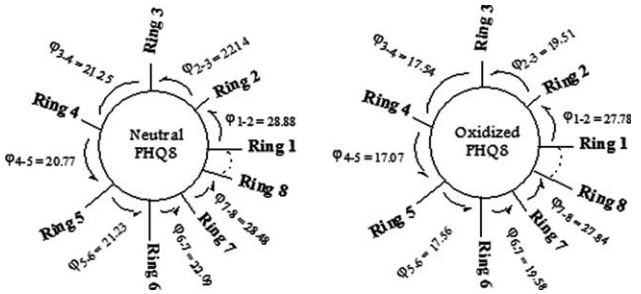

Scheme 3 Schematic representation of conformational structures of neutral and oxidized PHQ8 (the dihedral angles are expressed in degree).

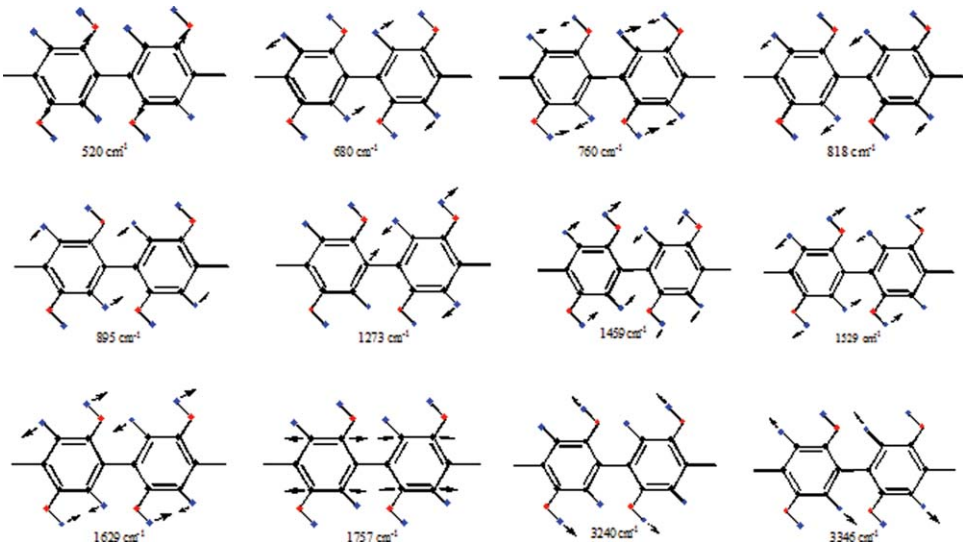

Figure 13 Approximate vibrational modes of PPHQ polymer. [Color figure can be viewed in the online issue, which is available at www.interscience.wiley.com.]

performed at the B3LYP/3-21G* level give a well-correlated optical properties with available absorption data. In contrast, HF calculations are not precise enough to obtain accurate optical properties for polyhydroquinone. In fact, the same HOMO–LUMO gap ($\sim$ 3 eV) value agrees qualitatively well with the experimental optical gap (2.62 eV). Therefore, we deduce that HOMO/LUMO level positions are quite similar. The optical shift between neutral and oxidized state allows probably for the mixing of σ and π orbital leading to a large band gap. At this stage, it is reasonable to consider PHQ8 oligomer as the model structure of PPHQ polymer. The corresponding optimized structures of the neutral and oxidized states are shown in Figures 9 and 10, respectively.

The frontier HOMO and LUMO plots of the PHQ8 optimized structures are shown in Figure 11. The dramatic decreases in LUMO and HOMO energies of the oxidized PHQ8 when compared with those of neutral state are consistent with the molecular orbital plots, in which the oxygen atom contributes significantly to LUMO. This implies that changes in LUMO/HOMO levels may be expected upon oxidation and consequently the reduction of the energy gap.

In an attempt to support this hypothesis and to confirm the experimental infrared assignments of the PPHQ polymer, we have theoretically studied its vibrational properties using the semiempirical AM1 method. In Figure 12, we compare the experimental

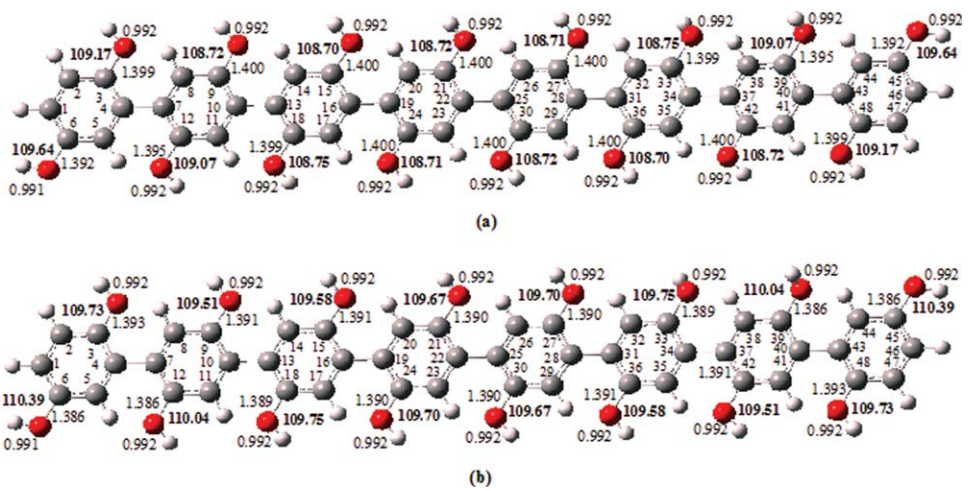

Figure 14 Model structure with numbering atoms of: (a) neutral and (b) oxidized PHQ8 (the C—O—H angle values expressed in degree, the C—O and O—H bond length values expressed in ångström). [Color figure can be viewed in the online issue, which is available at www.interscience.wiley.com.]

TABLE III
The Main Calculated Bond Lengths at the Neutral (First Line) and Oxidized (Second Line) States of PHQ8 Oligomer Structure

Ring 1		Ring 2		Ring 3		Ring 4		Ring 5		Ring 6		Ring 7		Ring 8	
C_1—C_2	1.393	C_7—C_8	1.402	C_{13}—C_{14}	1.405	C_{19}—C_{20}	1.405	C_{25}—C_{26}	1.405	C_{31}—C_{32}	1.405	C_{37}—C_{38}	1.405	C_{43}—C_{44}	1.402
	(6.543)		(6.192)		(6.121)		(6.111)		(6.109)		(6.110)		(6.115)		(6.191)
	1.390		1.400		1.406		1.408		1.408		1.408		1.408		1.404
	(6.525)		(6.245)		(6.068)		(6.011)		(6.001)		(5.995)		(6.008)		(6.139)
C_2—C_3	1.392	C_8—C_9	1.389	C_{14}—C_{15}	1.388	C_{20}—C_{21}	1.388	C_{26}—C_{27}	1.388	C_{32}—C_{33}	1.388	C_{38}—C_{39}	1.389	C_{44}—C_{45}	1.394
	(6.422)		(6.399)		(6.406)		(6.411)		(6.418)		(6.408)		(6.387)		(6.305)
	1.393		1.388		1.385		1.384		1.384		1.384		1.385		1.393
	(6.390)		(6.402)		(6.486)		(6.515)		(6.524)		(6.514)		(6.475)		(6.349)
C_3—C_4	1.419	C_9—C_{10}	1.414	C_{15}—C_{16}	1.414	C_{21}—C_{22}	1.415	C_{27}—C_{28}	1.414	C_{33}—C_{34}	1.414	C_{39}—C_{40}	1.412	C_{45}—C_{46}	1.392
	(5.690)		(5.843)		(5.848)		(5.838)		(5.839)		(5.849)		(5.911)		(6.490)
	1.422		1.423		1.425		1.426		1.426		1.426		1.422		1.396
	(5.582)		(5.564)		(5.510)		(5.486)		(5.481)		(5.499)		(5.606)		(6.365)
C_4—C_5	1.402	C_{10}—C_{11}	1.405	C_{16}—C_{17}	1.405	C_{22}—C_{23}	1.405	C_{28}—C_{29}	1.405	C_{34}—C_{35}	1.405	C_{40}—C_{41}	1.402	C_{46}—C_{47}	1.393
	(6.191)		(6.115)		(6.110)		(6.109)		(6.111)		(6.121)		(6.192)		(6.543)
	1.404		1.408		1.408		1.408		1.408		1.406		1.400		1.390
	(6.139)		(6.008)		(5.995)		(6.001)		(6.011)		(6.068)		(6.245)		(6.625)
C_5—C_6	1.394	C_{11}—C_{12}	1.389	C_{17}—C_{18}	1.388	C_{23}—C_{24}	1.388	C_{29}—C_{30}	1.388	C_{35}—C_{36}	1.388	C_{41}—C_{42}	1.389	C_{47}—C_{48}	1.392
	(6.305)		(6.387)		(6.408)		(6.418)		(6.411)		(6.406)		(6.399)		(6.422)
	1.393		1.385		1.384		1.384		1.384		1.385		1.388		1.393
	(6.349)		(6.475)		(6.514)		(6.524)		(6.515)		(6.486)		(6.402)		(6.390)
C_1—C_6	1.392	C_7—C_{12}	1.412	C_{13}—C_{18}	1.414	C_{19}—C_{24}	1.414	C_{25}—C_{30}	1.415	C_{31}—C_{36}	1.414	C_{37}—C_{42}	1.414	C_{43}—C_{48}	1.419
	(6.490)		(5.911)		(5.849)		(5.839)		(5.838)		(5.848)		(5.843)		(5.690)
	1.396		1.422		1.426		1.426		1.426		1.425		1.423		1.422
	(6.365)		(5.606)		(5.499)		(5.481)		(5.486)		(5.510)		(5.564)		(5.582)
C_3—O	1.399	C_9—O	1.400	C_{15}—O	1.400	C_{21}—O	1.400	C_{27}—O	1.400	C_{33}—O	1.399	C_{39}—O	1.395	C_{45}—O	1.392
	(6.753)		(6.703)		(6.712)		(6.715)		(6.718)		(6.735)		(6.882)		(7.065)
	1.393		1.391		1.391		1.390		1.390		1.389		1.386		1.386
	(6.969)		(7.071)		(7.091)		(7.102)		(7.115)		(7.139)		(7.273)		(7.330)
C_6—O	1.392	C_{12}—O	1.395	C_{18}—O	1.399	C_{24}—O	1.400	C_{30}—O	1.400	C_{36}—O	1.400	C_{42}—O	1.400	C_{48}—O	1.399
	(7.064)		(6.883)		(6.736)		(6.719)		(6.715)		(6.712)		(6.703)		(6.753)
	1.386		1.386		1.389		1.390		1.390		1.391		1.391		1.393
	(7.330)		(7.273)		(7.141)		(7.117)		(7.102)		(7.091)		(7.071)		(6.969)
C_4—C_7	1.487	C_{10}—C_{13}	1.485	C_{16}—C_{19}	1.484	C_{22}—C_{25}	1.484	C_{28}—C_{31}	1.484	C_{34}—C_{37}	1.485	C_{40}—C_{43}	1.487		
	(4.948)		(4.962)		(4.967)		(4.963)		(4.967)		(4.962)		(4.948)		
	1.481		1.473		1.471		1.471		1.471		1.473 5(5.208)		1.481		
	(5.082)		(5.208)		(5.246)		(5.250)		(5.246)				(5.082)		

The values written in parentheses, expressed in millidyne/ångström, represent the calculated force constants.

TABLE IV
Electronic Spin Densities and Charges Distribution of the Oxidized PHQ8 Oligomer Structure

Carbon	Spin density	Charge	Carbon	Spin density	Charge	Carbon	Spin density	Charge	Carbon	Spin density	Charge
1	0.034	−0.205	13	0.055	0.008	25	0.044	0.006	37	0.018	0.001
2	−0.014	−0.207	14	−0.026	−0.233	26	−0.020	−0.237	38	−0.010	−0.230
3	0.031	0.283	15	0.041	0.301	27	0.032	0.302	39	0.014	0.300
4	−0.004	−0.010	16	0.036	0.004	28	0.048	0.007	40	0.061	0.011
5	0.003	−0.185	17	−0.016	−0.234	29	−0.022	−0.237	41	−0.029	−0.219
6	−0.003	0.288	18	0.026	0.301	30	0.035	0.303	42	0.050	0.300
7	0.061	0.011	19	0.049	0.007	31	0.036	0.004	43	−0.004	−0.010
8	−0.029	−0.220	20	−0.022	−0.235	32	−0.016	−0.236	44	0.003	−0.184
9	0.050	0.297	21	0.035	0.302	33	0.026	0.301	45	−0.004	0.288
10	0.018	0.001	22	0.043	0.005	34	0.055	0.009	46	0.034	−0.205
11	−0.010	−0.230	23	−0.019	−0.237	35	−0.026	−0.234	47	−0.014	−0.206
12	0.014	0.300	24	0.031	0.302	36	0.041	0.302	48	0.031	0.283

and the theoretical infrared absorption spectra of oxidized PPHQ. The theoretical frequencies of different vibrational modes agree well with experimental data in the range of 400–4000 $cm^{-1.}$ The additional feature, which appears theoretically at 1760 cm^{-1}, was attributed to the stretching mode of the C=C bonds of the central ring of oligomer. In addition, we have reported the derived theoretical vibrational modes of PPHQ polymer in Figure 13.

In the following sections, we restrict our analysis to PHQ8 oligomer, a model structure of PPHQ polymer.

To investigate the effect of $TiCl_4$ on the properties of PPHQ polymer, we have compared the geometric parameters including bond length, dihedral angle, and vibrational properties such as force constants of oxidized PHQ8 to those of neutral state (Scheme 3, Fig. 14 and Table III). Theoretical calculations show that the oxidized PHQ8 oligomer structure becomes more planar, that is, the dihedral angle between successive *p*-hydroquinone decreases considerably (Scheme 3). On the other hand, progressive decreases in the bond length of C—C inter-rings occur as we move toward the center of the system (Fig. 14). Note that hydroxyl groups are coplanar with the phenyl rings whatever the state is. In addition, the hydroxyl bond lengths are not affected (d_{O-H} = 0.992 Å), whereas the C—O—H angles are slightly increased upon oxidation. These changes are probably originating from the hydrogen atoms interaction.

DISCUSSION

PPHQ was prepared by chemical oxidation using $TiCl_4$ as an oxidant. Infrared absorption and CPMAS ^{13}C-NMR analyses provide important information on the structure of PPHQ polymer. The latter was thermally stable up to 400 K and presents an optical gap at around 2.6 eV.

To better describe the polymer structure, we have performed theoretical calculations within *ab initio* DFT and semiempirical AM1 methods. From DFT calculations, we have demonstrated that with oligomer containing eight repetitive units of hydroquinone (PHQ8), it is possible to predict PPHQ polymer properties. This assumption was tested by evaluating HOMO–LUMO gap and vibrational properties, where different vibrational modes are assigned. Then, we have restricted our theoretical studies to the oxidized optimized oligomer structure, to describe the $TiCl_4$ effect on the properties of PPHQ polymer. Note that geometries optimization of neutral PHQ8 and PHQ9 were computed also with HF method for the sake of comparison. The DFT results of the present calculations are in excellent agreement with experimental data.

By analyzing the conformational structure of the neutral and oxidized state of PHQ8 oligomer, DFT calculations show that oxidation affects the planarity of the polymer lattice. Furthermore, it is well known that the physics of polyconjugated molecular systems is dominated by the delocalized π-electrons along the chain. In our case, the presence of EPR signal at room temperature indicates the creation of paramagnetic radical species during polymerization process. Therefore, we have also showed that the corresponding line width of its signal decreases with increasing temperature. This phenomenon was explained in terms of mobility of charge carriers (paramagnetic radical center), as it is often observed in the case of other conjugated polymers.[32]

From the electronic spin densities and charge distributions over the oxidized oligomer chain [Fig. 14(b) and Table IV], we conclude that negative spin densities and charges are located on CH aromatic, whereas positive values are obtained for carbon attached to the hydroxyl groups. This segregation supports well the CPMAS ^{13}C-NMR spectrum by the presence of two corresponding domains of chemical shift. Consequently, a correlation between structural properties and DFT calculations is obtained, and then, the shielding or unshielding of aromatic carbon chemical shifts is strictly related to the electronic population already discussed.

CONCLUSIONS

This article shows the effective complementary of the experimental studies and theoretical calculations including *ab initio* DFT and semiempirical AM1 methods to obtain a detailed structure–property relationship of PPHQ prepared by chemical oxidation in the presence of $TiCl_4$ as an oxidant. The correlation between different results demonstrates that PPHQ is structurally homogenous and stable up to 400 K. Second, oligomer with eight repeat units (PHQ8) is chosen as the model structure for predicting the observed optical, vibrational, and structural properties of PPHQ polymer.

From an application point of view, it is very important to obtain information about the electronic structure and the optical properties of the PPHQ polymer. Finally, following these encouraging results, a much efforts have been undertaken in our laboratory to develop organic electronic devices based on this polymer.

References

1. Berlin, A. A.; Ragimov, A. V.; Zade, S. I. S.; Gadzhieva, T. A.; Takhmazov, B. M. Vysokomol Soyed 1975, 17, 111.
2. Furlani, A.; Russo, M. V.; Cataldo, F. Synth Met 1989, 29, E507.
3. Yamamoto, K.; Asada, T.; Nishide, H.; Tsuchida, E. Bull Chem Soc Jpn 1990, 63, 1211.
4. Yamamoto, T.; Kimura, T. Macromolecules 1998, 31, 2683.
5. Lee, W. E.; Brown, E. R. In The Theory of the Photographic Process, 4th ed.; James, T. H., Ed.; Macmillan: New York, 1977; Chapter 11, pp 291–334.
6. Ayachi, S.; Bouzakraoui, S.; Hamidi, M.; Bouachrine, M.; Molinié, P.; Alimi, K. J Appl Polym Sci 2006, 100, 57.
7. Mabrouk, A.; Alimi, K.; Molinié, P.; Nguyen, T. P. J Phys Chem B 2006, 110, 1141.
8. Zojer, E.; Cornil, J.; Leising, G.; Brédas, J. L. Phys Rev B 1999, 59, 7957.
9. Bouachrine, M.; Lère Porte, J. P.; Moreau, J. J. E. Phosphorus Sulfur Silicon Relat Elements 1999, 152, 265.
10. Bouachrine, M.; Lère Porte, J. P.; Moreau, J. J. E.; Chi Man, M. W. J Mater Chem 1995, 5, 797.
11. Metz, G.; Wu, X.; Smith, S. O. J Magn Reson 1994, 110, 219.
12. Bennett, A. E.; Rienstra, C. M.; Auger, M.; Lakshmi, K. V.; Griffin, R. G. J Chem Phys 1995, 103, 6951.
13. Frisch, M. J.; Trucks, G. W.; Schlegel, H. B.; Scuseria, G. E.; Rubb, M. A.; Cheeseman, J. R.; Zakrzewski, V. G.; Montgomery, J. A.; Stratmann, R. E.; Burant, J. C.; Dapprich, S.; Millam, J. M.; Daniels, A. D.; Kudin, K. N.; Strain, M. C.; Farkas, O.; Tomasi, J.; Barone, V.; Cossi, M.; Cammi, R.; Mennucci, B.; Pomelli, C.; Adamo, C.; Clifford, S.; Ochterski, J.; Petersson, G. A.; Ayala, P. Y.; Cui, Q.; Morokuma, K.; Malick, D. K.; Rabuck, A. D.; Raghavachari, K.; Foresman, J. B.; Cioslowki, J.; Ortiz, J. V.; Stefanov, B. B.; Liu, G.; Liashenko, A.; Piskorz, P.; Komaromi, I.; Gomperts, R.; Martin, R. L.; Fox, D. J.; Keith, T.; Al-Laham, M. A.; Peng, C. Y.; Nanayakkara, A.; Gonzalez, C.; Challacombe, M.; Gill, P. M. W.; Johnson, B. G.; Chen, W.; Wong, M. W.; Andres, J. L.; Head-Gordon, M.; Replogle, E. S.; Pople, J. A. GAUSSIAN 98; Gaussian Inc.: Pittsburgh, PA, 1998.
14. Becke, A. D. J Chem Phys 1993, 98, 5648.
15. Lee, C.; Yang, W.; Parr, R. G. Phys Rev B 1998, 37, 785.
16. Pietro, W. J.; Francl, M. M.; Hehre, W. J.; Defrees, D. J.; Pople, J. A.; Binkley, J. S. J Am Chem Soc 1982, 104, 5039.
17. Pickholz, M.; Dos Santos, M. C. Synth Met 1999, 101, 528.
18. Dicésare, N.; Belletête, M.; Marrano, C.; Leclerc, M.; Durocher, G. J Phys Chem A 1998, 102, 5142.
19. Dewar, M. J. S.; Zoebish, E. G.; Healy, E. F.; Stewart, J. J. P. J Am Chem Soc 1985, 107, 3902.
20. Stewart, J. J. P. Quantum Chemistry Program Exchange No. 455; MOPAC 2000 © Fujitsu limited: Tokyo, Japan, 1999.
21. Guarrera, D.; Taylor, L. D.; Warner, J. C. Chem Mater 1994, 6, 1293.
22. Mizoguchi, K. Synth Met 2001, 119, 35.
23. Kahhol, P. K.; Pinto, N. J. Synth Met 2004, 140, 269.
24. Kahhol, P. K.; Pinto, N. J. Solid State Commun 2002, 124, 195.
25. Lin-Vien; Grasselli, J. G.; Colthup, N. B. Handbook of Infrared and Raman Characteristics Frequencies of Organic Molecules; Academic Press, Harcourt Brace Jovanovich Publishers: New York, 1989.
26. Pavia, D. L.; Lampman, G. M.; Kriz, G. S. Introduction to Spectroscopy; Saunders College: Philadelphia, 1979.
27. Ayachi, S.; Alimi, K.; Bouachrine, M.; Hamidi, M.; Mevellec, J. Y.; Lère-Porte, J. P. Synth Met 2006, 156, 318.
28. Liu, T.; Gao, J.-S.; Xia, B.-H.; Zhou, X.; Zhang, H.-X. Polymer 2007, 48, 502.
29. Yang, L.; Feng, J.-K.; Ren, A.-M.; Sun, J.-Z. Polymer 2006, 47, 1397.
30. Yang, L.; Feng, J.-K.; Ren, A.-M. Polymer 2005, 46, 10970.
31. Yang, L.; Feng, J.-K.; Liao, Y.; Ren, A.-M. Polymer 2005, 46, 9955.
32. Demirboga, B.; Önal, A. M. J Phys Chem Solids 2000, 61, 907.